PROYECTOS INSTITUCIONALES
Y
DE VINCULACIÓN

UANL
UNIVERSIDAD AUTÓNOMA DE NUEVO LEÓN

FIME
FACULTAD DE INGENIERÍA MECÁNICA Y ELÉCTRICA

CAVITY-RATE ANALYSIS APPLIED TO THE FREQUENCY OSCILLATIONS RELAXATION IN A SELF-PULSED, LARGE-MODE-AREA YTTERBIUM-DOPED FIBRE LASER

Daniel Toral-Acosta
Facultad de Ciencias Físico Matemáticas, Universidad Autónoma de Nuevo León, Pedro de Alba S/N, Ciudad Universitaria, San Nicolás de los Garza, NL, 66450, México
toralacostadaniel@gmail.com

Romeo Selvas-Aguilar
Facultad de Ciencias Físico Matemáticas, Universidad Autónoma de Nuevo León, Pedro de Alba S/N, Ciudad Universitaria, San Nicolás de los Garza, NL, 66450, México
rselvas@gmail.com

Mario Alberto García-Ramírez
Facultad de Ingeniería Mecánica y Eléctrica, Universidad Autónoma de Nuevo León, Pedro de Alba S/N, Ciudad Universitaria, San Nicolás de los Garza, NL, 66450, México.
seario@gmail.com

ABSTRACT

In this work, an analysis for a self-pulsing behavior within a large-mode-area Ytterbium-doped fibre laser operated as a free running laser is presented. A set of equations that describes the relaxation oscillations frequency by considering a cavity as well as the atomic rate equations were obtained. In here, the behaviour of the self-pulsing is due to the un-pumped fibre section that plays a key role for the saturate absorber. Analytical results depicts that instead of reaching a continuous wave-based regime, the laser output will show pulses with an increasing repetition rate due to the pump power is higher. It is in good agreement with the natural behaviour observed within this fibre laser.

KEYWORDS: Inteference Effect, Laser Dynamics, Fibre Laser.

INTRODUCTION

Double-clad rare-earth doped-fibre structures were developed in order to overcome the limitations at the output power level imposed by the difficulty to pump the doped core of a single mode fibre structures [1-3]. After reaching significant power levels, in the level of tens of Watts [1-3], nonlinear effects start to play a significant role. Since the strength of nonlinear effects depends inversely on the doped core area, additional scaling of the output power level requires to improve the design of large mode area (LMA) structures [4].

As a consequence, it increases the threshold for the stimulated Raman scattering and allows to increase the dopant concentration. In general, a LMA fibre structure, by nature, supports the propagation of a few modes inside the fibre. Since it is always desired to have an output laser beam with the highest spatial quality, i.e. diffraction limited beam. It means to force the laser oscillation into a single transverse mode is used, for example, by tapering fibre sections [5]. For a few applications a rather high beam quality is required. Nevertheless, a rich dynamics are keen to be studied and characterized when the laser output beam is the result of the interaction between several modes that supports the fibre core. The effect of multiple longitudinal and transverse modes supported by the fibre laser enhance such effects as the laser wavelength is swept [6,7], closely correlated with the laser pulsed operation where the laser, around the threshold, self-pulses due to a saturable absorption effect by un-pumped fibre sections and after an increased pump power, the Brillouin effect may reach the threshold for stimulated Raman scattering which at the end results in a chaotic pulsed output.

The dynamics of self-pulsing and self-sweeping in Yb-doped fibre (YDF) lasers have been studied under several conditions [6-9]. An interesting explanation to these attributes highlights the presence of dynamical gratings in the YDF that are produced by the standing wave of the oscillating laser signal within a Fabry-Perot cavity [6-8]. Alternatively in [8], it is shown that a dynamical grating is produced by weak interference of the laser signal. It reflects the signal at the output coupler in a ring-cavity configuration. Finally in [9] a side pumped Fabry-Perot laser setup with a bad cavity configuration, the pulsed regime near threshold is attributed to re-absorption of laser signal in un-pumped sections of the YDF.

The relaxation oscillations in a laser is a behaviour that leads to self-pulsing in which at threshold, the laser output start to show a characteristic transient or modulation behaviour [10-11]. This is common to several types of lasers, including most solid state lasers, semiconductor lasers and other laser devices in which the recovery time of the excited state population inversion is substantially longer than the cavity decay time [12]. In some cases, when continuous wave operation is required, it can be added appropriate lengths of passive fibre to the laser cavity [10,11]. By increasing this way, the cavity lifetime of the photons circulating inside the laser cavity and suppressing the pulsed laser output decreases. On the other hand, when pulsed operation is desired (as occurs in mostly Q-switched lasers), there are added inside the laser cavity optical elements that produce losses in a periodic fashion [1-3].

In this work, it is presented an analysis based on the cavity and atomic rate equations to obtain the frequency of the relaxation oscillations of a large-mode-area Ytterbium-doped fibre laser (LMA-YDFL) operated as a free running laser. The aim of the afore mentioned analysis is to explain the self-pulsed regime experimentally observed (starting from lasing threshold) in the LMA-YDFL under all levels of optical pump power up to a maximum available pump power of 20 W. The repetition rate of the laser pulses gets increased as the pump power is done. In this experiment, it was not observed any non-linear effect related to stimulated Raman scattering nor stimulated Brillouin scattering. For that reason it was not necessary to consider these effects in the present analysis. Is worth mentioning the fact that the large-mode-area structure of the fibre, allows the propagation o several modes in the doped core, resulting in the presence of traverse hole burning in which the gain seen by each mode is different. It allows the simultaneous operation at different laser wavelengths producing an irregular pulsing behaviour.

EXPERIMENTAL SETUP.

The experimental setup consists of a simple linear, or Fabry-Perot, laser cavity formed by reflections at the two fibre ends (free running laser), and additional optical elements to collimate (lenses) and separate the pump from the laser wavelength (dichroic mirrors). The fibre used to build the cavity is a commercial fibre 20/400 LMA-YDF from LIEKKI and the pump source was a fibre coupled Coherent laser diode with maximum pump power of 40 W. In the implementation of the fibre laser only a fraction of the pump power was used (less than 20 W). At the time of realising the experiments we had no means to cool the fibre ends to avoid the glass breaking due to the thermal load caused by the end pumping. The dichroic mirrors at the input and output ends have a high transmission at the pump wavelength and high reflection at the laser wavelength (which is around 1070 nm). Thus most of the measured signals by the power meter, optical spectrum analyzer (OSA), and photodetector-oscilloscope correspond to the laser or ASE power. It is worth to mention that the signal entering the OSA was collected through a single mode fibre (980HP from Nufern), so that a possible interference between the distinct modes supported by the LMA-YDF, which may occur inside the spectral analyzer is avoided. This is important to mention, since the OSA measures a modulated ASE signal, which in this particular case is due to the mode mixing occurring inside the active fibre. By using a Vytran precision cleaver, both fibre ends were perpendicularly cleaved, so that, approximately a 4% Fresnel reflection was obtained from both ends. This 4% may be overestimated, since there is a high probability that the distinct transverse modes, particularly the higher order modes, experience a lower back reflection.
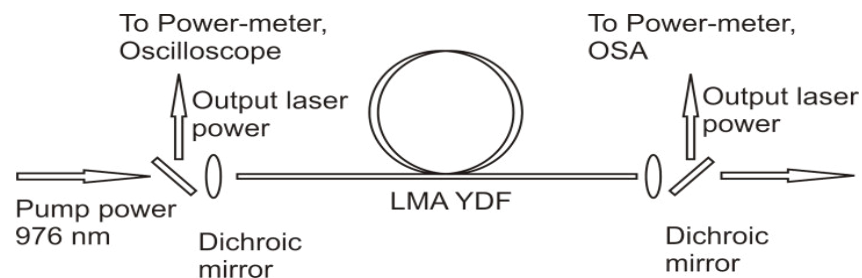

Figure 1. Sketch of the experimental setup, here, the cavity mirrors are simply constructed by the Fresnel reflectivity at the cleaved fibre ends. The generated laser signal inside the active fibre is bi-directional, producing output laser beams at the two fibre ends. The dichroic mirrors have high transmission at the pump wavelength and high reflectivity at the signal wavelength, thus, the signals measured by the power-meter, optical spectrum analyzer and photo-detector correspond mostly to the laser signal.

MODELING OF SELF-PULSING MECHANISM.

Below there is list of some of the parameters that are relevant for the dynamics of self-pulsing [12]:

Cavity length: L=4 m
Round trip time: T=2nL/c= 38.6667 ns, which corresponds to a free-spectral range
          frequency of 25.86 MHz, assuming a core refractive index n=1.45

Fractional power losses due to out-coupling □c:

$$\delta_c = \ln(1/(0.04*0.04)) = 2.54593$$

Cavity lifetime □c=T/□c:

$$\tau_c = 15.1876 ns$$ (no active ions present)

In order to obtain the frequency of the relaxation oscillations, we derive the coupled cavity and atomic equations relevant for our laser system. Similar to reference [13], it is assumed that the Yb3+ is a two-level system without the excited state absorption and that the interactions and polarization effects between neighbouring ions are negligible. The last assumption is reasonable, since in our experiments we did not observe any effects such as photo-darkening which may be an indication of clustering, hence it is assumed that the self-pulsing is entirely due to saturable absorption from un-pumped sections.

Now we consider the critical pump power to obtain a gain coefficient of zero and the relation governing the evolution of the pump power along a doped fibre [14]:

$$P_{p,cr} = \frac{h v_p A_{clad}}{\left(\dfrac{\sigma_{a,p}\sigma_{e,s}}{\sigma_{a,s}} - \sigma_{e,p}\right)\tau} \tag{1}$$

$$\ln \frac{P_p(z)}{P_p(0)} \div + \frac{P_p(z)}{P_{p,sat}} \frac{P_p(0)}{} + N_{a,p} z = 0 \tag{2}$$

where:

$$P_{p,sat} = \frac{h v_p A_{clad}}{(\sigma_{a,p} + \sigma_{e,p})}$$

and N is the total concentration of ions, assumed to be uniform along the active fibre core, =Acore/Aclad is the ratio between the core and cladding areas, and it is assumed that the dopant profile coincides with the transverse distribution of the laser light propagating through the core. Here the subscripts a, e, p, and s, in the □'s cross-sections stands for absorption, emission, pump and laser, respectively.

Additionally as shown elsewhere [14] the corresponding single pass power gain exponent in a fibre length L is given by:

$$\exp\left(\int_0^L g(z)dz\right) = \frac{\phi_p\left(\sigma_{e,s} + \sigma_{a,s}\right)\tau P_a}{A h v_p} - N\sigma_{a,s}L \tag{3}$$

Where: $P_a = P_p(0) - P_p(L)$

As it has been mentioned, the mechanism responsible for the self-pulsing most probably comes from the un-pumped section of the fibre that acts as a saturable absorber. If we take the point where the un-pumped fibre starts to be a saturable absorber section as the point where the pump power is equal to the critical pump power, then it is possible to find the corresponding length by solving (2), with Pp(z) substituted by Pp,cr, and by employing the cross sections for absorption/emission of the corresponding pumping and laser wavelengths.

The active fibre considered in this work has a core/cladding diameter of 20/400 $\Box$m. It is assumed that the fibre has a concentration of 2x1020 ions/cm3, a fluorescence lifetime of 1.5 ms, equal absorption and emission cross sections at the pump wavelength of 980 nm of 2.5x10-24 m2, absorption and emission cross-sections at the laser signal wavelength (at $\Box\, 1055nm$) of 6.59x10-27 m2 and 0.312x10-27m2, respectively.

Figure 2 shows a plot of the transparency length as a function of the input pump power. In plotting this graph we have substituted the factor $\Gamma\, N\sigma_{a,p}$ by an effective multimode absorption of 0.7 dB/m, which is a typical value for commercial LMA double-clad Yb-doped fibres. As it is shown in the plot, as the pump power increases, the zero gain length increases, thus, reducing the saturable absorption length.

The impact of the mentioned saturable absorption length on the pulsing behaviour is the following: In terms of the cavity lifetime the saturable absorption section acts as loss mechanism, just as the output coupling mirrors and background loss that both reduce the photon lifetime that is one of the main factors controlling the pulsing behaviour. It is important to notice that also the way in which the fibre is wrapped affects the pump absorption, and in fact the real values may deviate significantly from the ones shown in figure 2, i.e., more pump power may be needed to reach transparency at a given fibre length.
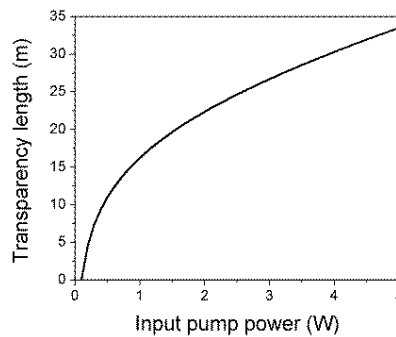

Figure 2. Transparency length needed to get a coefficient gain of zero as a function of input pump power.

Now consider the following general inversion and cavity rate equations [12], applicable for modelling our laser

$$\frac{dn_s(t)}{dt} = KN_2(t)(n_s(t)+1) - \gamma_c n_s(t) \tag{4}$$

$$\frac{dN_u(t)}{dt} = R_p - KN_u(t)n_s(t) - \frac{N_u(t)}{\tau} \tag{5}$$

where Rp is the pump rate, Nu is the population of the upper laser level, n_s is the number of cavity photons, and τ is the upper level lifetime. As can be observed, these two coupled equations are non-linear because of the product terms $KN_u(t)n_s(t)$, and as a consequence, exhibiting relaxation oscillations in their evolution toward a steady state. However, when the strong spiking has damped to small amplitude oscillations around the steady state, it can be shown by a linearized analysis [12] of the equations (4) and (5), that the frequency and damping of the relaxation oscillations can be given by the solution of the linearized system:

$$\left.\begin{array}{l} \dfrac{dn_s(t)}{dt} = (r-1)\gamma_2 N_u(t) \\[2mm] \dfrac{dN_u(t)}{dt} = -\gamma_c n_1(t) - r\gamma_2 N_u(t) \end{array}\right\} \tag{6}$$

Where $\gamma_2 = 1/\tau$, $r = \tau R_p / N_{u,th}$. Is worth mentioning that in the linearization process, the coupled system (6) is expressed in terms of the steady state or dc solutions of the system (4) and (5) given by:

$$\left.\begin{array}{l} n_s^{ss} = (r-1)/K\tau \\[2mm] N_{u,th} = \gamma_c / K; with: \gamma_c = \delta_c / T \end{array}\right\} \tag{7}$$

The solution of the system (6) is determined by the characteristic equation $s^2 + r\gamma_2 s + (r-1)\gamma_2\gamma_c = 0$ whose natural roots give the exponential decay rates and oscillation frequencies of the relaxation oscillation behaviour. In the case of solid state lasers it can be shown that [12]:

$$s_1, s_2 \approx \frac{r\gamma_2}{2} \pm j\sqrt{(r-1)\gamma_2\gamma_c - \left(\frac{r\gamma_2}{2}\right)^2} = -\gamma_{sp} \pm j\omega'_{sp} \tag{8}$$

This leads to a damped sinusoidal response (evolution of cavity photons population) in the form [12]:

$$n(t) = n_s^{ss} + n_1 e^{-\gamma_{sp}t} \cos(\omega'_{sp}t) \tag{9}$$

Considering the fact that in solid state lasers the atomic decay γ_2 rate is very much slower compared to the cavity decay rate γ_c we have: $_c \gg_2$. For this reason, and from equation (8), it can be shown that the frequency of these spikes or pulses is given by [12]:

$$\omega_{sp} = \sqrt{(r-1)\gamma_2\gamma_c} = \sqrt{(r-1)\gamma_c/\tau}$$

(10)

In order to apply the results for the steady state values of (4) and (5) and the earlier explained formulas for the frequency of the relaxation oscillations, we need to find the corresponding values of K and RP for our case (assuming the conditions of saturable absorption from un-pumped sections of the LMA fibre). For the particular case of pumping at 980 nm, assuming that the population of the lower laser level is negligible due to a fast relaxation to the ground level, the population of the upper laser level Nu may be written as:

$$\frac{dN_u}{dt} = \left(\frac{\sigma_{a,p}P_p}{h\nu_pA_{clad}}\right)N - \left(\frac{\sigma_{e,s}c}{2A_{core}L_{tot}}\right)n_sN_u - \left(\frac{2h\nu_pA_{clad}+(\sigma_{a,p}+\sigma_{e,p})P_p}{h\nu_pA_{clad}\tau}\right)N_u$$

(11)

From here, we identify:

$$R_p \to \left(\frac{\sigma_{a,p}P_p}{h\nu_pA_{clad}}\right)N \qquad K \to \left(\frac{\sigma_{e,s}c}{2A_{core}L_{tot}}\right) \quad \text{and} \quad \tau \to \left(\frac{h\nu_pA_{clad}\tau}{2h\nu_pA_{clad}+(\sigma_{a,p}+\sigma_{e,p})P_p}\right)$$

In order to find the modification in the γ_c factor appearing in Eq. (4), let us consider the single pass gain for the laser signal until the transparency length Ltr. At this point, the signal laser power will be equal to the laser power at the input point, i.e., Ps(Ltr)=Ps(0). Further propagation through the absorbing fibre section will reduce the laser signal power according to the following approximated formula:

$$P_s(L_{tot}) = P_s(0)\exp\left[-\left(\sigma_{a,s}N+\alpha_s\right)L_{up}\right]$$

(12)

where the un-pumped length is Lup=Ltot-Ltr. On writing this equation we have assumed that all the atoms on the remaining fibre section are on the ground state. For the purpose of deriving the cavity rate equations let us assume that the populations on each section are uniform along their length, so that, considering equation (3) in a single pass the laser power gain may be written as [14]:

$$P_s(L_{tot}) \approx P_s(0) \exp\left[\frac{\sigma_{e,s}+\sigma_{a,s}}{A_{clad}hv_p}\tau P_a - \alpha_s L_{tr}\right]\exp\left[-(\sigma_{a,s}N+\alpha_s)L_{up}\right]$$

(13)

where $P_a = P_p(0)-P_{p,cr}$. Following [12], after a round trip the exponential gain is squared (double-pass gain), and the mirror reflection coefficients are included, if we consider this occurs at a time t=0, it may be written as:

$$P_s(T) = P_s(0)R_1 R_2 \exp\left[2\left(\frac{\sigma_{e,s}+\sigma_{a,s}}{A_{clad}hv_p}\tau P_a - \alpha_s L_{tr}\right)\right]\exp\left[-2(\sigma_{a,s}N+\alpha_s)L_{up}\right]$$

(14)

After m round trips we will have:

$$P_s(mT) = P_s(0)\left\{e^{\left(2\frac{\sigma_{e,s}+\sigma_{a,s}}{A_{clad}hv_p}\tau P_a\right)}e^{(-2\sigma_{a,s}NL_{up})}R_1 R_2 e^{(-2\alpha_s L_{tot})}\right\}^m = P_s(0)e^{2m\frac{\sigma_{e,s}+\sigma_{a,s}}{A_{clad}hv_p}\tau P_a}e^{-2m\sigma_{a,s}NL_{up}}e^{-m\delta_c}$$

Where $L_{tot} = L_{up}+L_{tr}$ and $\delta_c = 2\alpha_s L_{tot}+\ln\left(\frac{1}{R_1 R_2}\right)$. By substituting m=t/T,

$$P_s(t) = P_{s,0}e^{(\gamma_{tr}-\gamma_{up}-\gamma_c)t}$$

(15)

Where we have defined: $\gamma_{tr} = \dfrac{2\dfrac{\sigma_{e,s}+\sigma_{a,s}}{A_{clad}hv_p}\tau P_a}{T}$, $\gamma_{up} = \dfrac{2\sigma_{a,s}NL_{up}}{T}$ and $\gamma_c = \dfrac{\delta_c}{T}$

After differencing (15) with respect to time we obtain the relationship:

$$\frac{dP_s(t)}{dt} = \left(\gamma_{tr}(t)-\gamma_{up}(t)-\gamma_c(t)\right)P_s(t)$$

(16)

and now the ▢c factor includes the effect of the un-pumped section by the substitution:

$$\gamma_c \rightarrow \gamma_c+\gamma_{up} = \frac{\delta_c+2\sigma_{a,s}NL_{up}}{T}$$

(17)

The steady state solutions to the inverted population and the photon density can now be written by considering equations (7), (11) and (17) as [12]:

$$N_{2,th} = \frac{\gamma_c}{K} = \frac{2A_{core}L_{tot}(\delta_c + 2\sigma_{a,s}N L_{up})}{T\sigma_{e,s} c} \tag{18}$$

$$n_s^{ss} = \left(\frac{\tau R_p}{N_{2,th}} - 1\right)\frac{1}{K\tau} = \frac{(r-1)}{K\tau} \tag{19}$$

where r is the pump rate:

$$r = \frac{(\tau T)(\sigma_{a,p}\sigma_{e,s}c)P_p N}{(2A_{core}L_{tot}(\delta_c + 2\sigma_{a,s}N L_{up})(2h\nu_p A_{clad} + (\sigma_{a,p} + \sigma_{e,p})P_p)} \tag{20}$$

By comparing equations (7) with (18) it is clear that one of the effects of the un-pumped section is to increase the necessary inversion to reach the laser threshold. In addition by employing in equation (10) the derived values for r, γ_c and τ (equations 20, 17 and 11 respectively) concerning to our case, the relaxation oscillation frequency will be given by:

$$\omega_r = \sqrt{(r-1)\frac{\gamma_c}{\tau}} = \sqrt{(r-1)\left(\frac{\delta_c + 2\sigma_{a,s}N L_{up}}{\tau T}\right)\left(2 + \frac{(\sigma_{a,p} + \sigma_{e,p})P_p}{h\nu_p A_{clad}}\right)} \tag{21}$$

Since r and Lup are interrelated, an increase in the pump rate means a reduction in the un-pumped length and hence a reduction in the frequency of the relaxation oscillations that may be screened by the additional contribution from the third multiplicative terms inside square root in Eq. (21). This is clearly in agreement with our experimental observations, where an increase in the pump power results in increasing the pulses repetition rate. The equations obtained above do not account for the presence of multiple longitudinal and transverse modes and their interaction. A more detailed and complicate analysis is needed in order to match the theory with the experimental results (see below); however this is not the aim of the present study, aimed on giving a rather general qualitative explanation of the effect of an un-pumped fibre section.

EXPERIMENTAL RESULTS.

We will describe here the dynamics of the laser performance above threshold, under different levels of optical pump power. Figure 2(a) shows the output laser power spectrum measured from one of the output ends of the LMA-YDFL (the right end in figure 1), at a current of 17 A of the pump diode. As can be observed a single laser line mounted on the amplified spontaneous spectrum (ASE) background is measured.

The ASE background shows a wavelength modulation, characteristic of an interference effect, which in this case may be caused by the modal beating between the modes supported by the fibre core. The spectrum was measured from the output of a single mode fibre with cutoff below the operation range of the laser, so that this spectral interference is non-apparatus related. In figure 2(b), is shown the time trace of the measured output laser power, demonstrating regular pulsing.

The mechanism responsible for the self-pulsing most probably comes from the un-pumped section of the fibre that acts as a saturable absorber. In terms of the cavity lifetime the saturable absorption section acts as loss mechanism, just as the output coupling mirrors and background loss that both reduce the photon lifetime that is one of the main factors controlling the pulsing behavior.
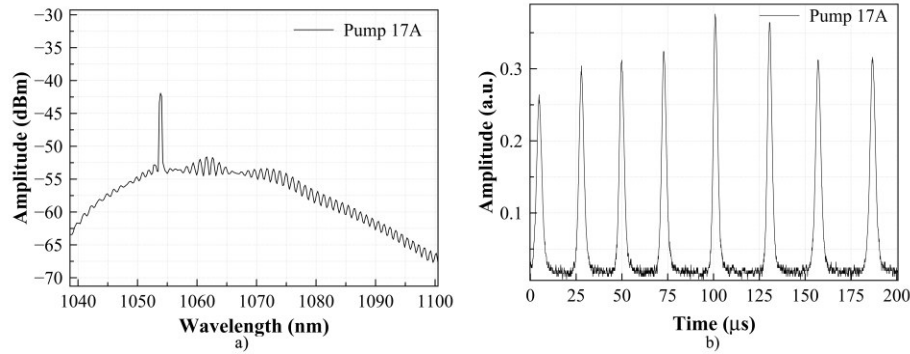

Figure 2. (a) and (b) Output laser power as a function of wavelength and time at a laser diode pump driver current of 17 A, measured by using an OSA and a photodetector- oscilloscope, respectively.

In this case, as observed in other reports [6] the laser wavelengths do not maintain stable positions in figure 2 (a). This was realised after reducing the wavelength span to zero at the shown wavelength and increasing the sweep rate of OSA, resulted in sudden changes in amplitude in excess of 10 dB. Since this wavelength sweeping was in the order of nanometers it was difficult to follow. A close view of the pulses generated at 17 A is shown in figure 3. The FWHM and repetition rate of the pulses are 3 microseconds and 33 kHz, respectively. Since the total power measured from both ends was 340 mW, the pulse energy and peak power are 10 microJoules and 3.4 W, respectively.
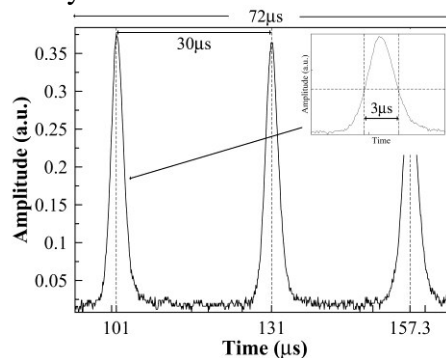

Figure 3. Close view of the pulses generated at 17 A pump diode driver current. The separation between pulses is 30 microseconds and the FWHM is 3 microseconds.

By increasing the pump-diode-driver current to 19 A, in appearance more laser lines are generated as shown on figure 4 (a); however, in this case it is more evident the jumps on the laser wavelength lines from sweep to sweep of the OSA, appearing and disappearing from time to time. Thus, with our current experimental measurements we cannot guaranty that all the laser lines are generated simultaneously or there is a single wavelength that jumps all over the gain

spectral range of the LMA-YDF. From the time trace of the output laser power shown in figure 4 (c), it can be observed a very irregular pulse generation, with varying amplitude and with not well-defined repetition rate. It is more similar to a chaotic pulse train generation, characteristic for circumstances where the Raman and Brillouin effects are simultaneously present with the self-pulsing; however, unlike to other reports of self-pulsing where the core is single-mode [15], in the present case, the pulsed energy corresponds to the wavelength region inside the fluorescence band of Yb. This could be explained by considering the fact that for the multimode core of our LMA-YDF, the onset of generation for the Brillouin and Raman effects is higher than in the single-mode case. Perhaps each measured wavelength on the left graphs may correspond to a single laser transient that cannot be measured fast enough by a common OSA and, as a consequence, the temporally pulses possibly are the superposition of several component pulses and each component may be associated with a particular laser wavelength generated at given time.
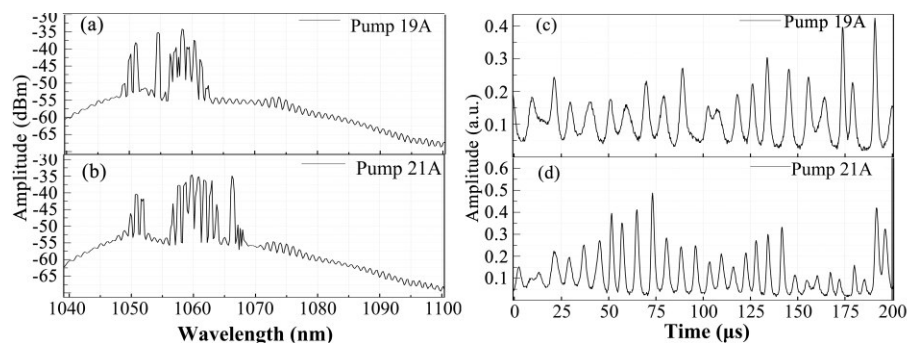

Figure 4. (a) and (b) Output laser power as a function of wavelength at a laser diode pump driver current of 19 A and 21A respectively, measured by using an OSA; (c) and (d) Time trace of the output laser power at a laser diode pump driver current of 19 A and 21A respectively, measured by using a photodetector- oscilloscope.

The above mentioned effects are much more apparent as the pump diode driver current is increased [Figures 4 (b) and (d)]. As it can be observed, the time traces show rather irregular pulses, characteristic of a transitory pulses or laser spikes. Further increment on the pump diode driver, the current increased the peak pulse power and heat the fibre ends at a level that resulted in the damage of the fibre ends, but not catastrophic, since the laser operation was recovered after re-cleaving the ends. It is worth to mention that in the case presented in this work there are longitudinal and transverse modes interacting, which make difficult and numerically expensive in modeling.

DISCUSSION.

In contrast with self-pulsing in double-clad YDF lasers where the core is single-mode [15], there is no noticeable generation of longer wavelength components as those corresponding to the stimulated Raman scattering process. It is evident that for our multimode core, the onset of cascaded Raman generation is significantly higher than in the single mode core case, so that the pulsed energy stay in the same wavelength region, i.e., inside the fluorescence band of Yb.

Another important difference observed is the fact that the generated ASE spectrum has a noticeable comb like shape modulation, which is the result of the interaction between the transverse modes supported by the fibre core. This means that the interference effects between the multiple modes have significant impact in the laser operation, since the laser wavelengths generally coincide with one of the peaks of the modulated ASE spectrum. This is also observed when a comb like filter is inserted into a fibre laser cavity [16].

The main impact of the presence of the multiple modes in the fibre core is the transverse spatial hole burning [17] which allows simultaneous laser operation at different wavelength regions, as noticed in the last section. In fact, temporally pulses appear to be the superposition of several component pulses, and each component may be associated with a particular laser wavelength generated at given time. This in agreement with the observation of laser wavelength sweeping around the laser threshold [6,7], where operation is a kind of pulsed regime and pulses are generated by the relaxation oscillations which are due to the presence of un-pumped saturable absorption sections, as it was demonstrated in Section 3. In our case, we have the advantage that the absence of nonlinear effects allows a clear picture of the relation between laser wavelength sweeping and pulsing. Nevertheless, though this relation is clear in our experiments, a theoretical explanation of the phenomenon is difficult, given the fact that we have added another degree of freedom, the interaction between the transverse and longitudinal modes inside the fibre laser cavity.

CONCLUSIONS.

We presented the characteristics of self-pulsing in a LMA-YDFL. The self-pulsing is shown to be produced by the saturable absorption present in not efficiently pumped active fibre sections. The presence of several transverse modes, in conjunction with the multiple longitudinal modes associated with each results in a transverse spatial hole-burning effect, which results in a difference in the gain seen by each mode. The latter allows the simultaneous operation at different laser wavelengths and producing an irregular pulsing behaviour, which becomes more and more irregular as the number of laser lines increases. The regular pulsing is only observed when a single laser wavelength is generated, however this laser line sweeps its position by a few nanometers.

Acknowledgments

REFERENCES.

[1] Sun W, Yu H J, Zhang L, Yan S L, Dong Z Y, Han Z H, Hou W, Li J M and Lin X C 2013 A high average power single-stage picosecond double-clad fiber amplifier Laser Phys. 23 095101 (4pp)

[2] Fang Q, Qin Y, Wang B and Shi W 2013 11 mJ all-fibre-based actively Q-switched fibre master oscillator power amplifier Laser Phys. Lett. 10 115103 (4pp)

[3] Zenteno L 1993 High Power Double Clad Fibre Lasers IEEE J. Lightwave Technol. 11 1435-1446

[4] Jeong Y, Sahu J K, Payne D N and Nilsson J 2004 Ytterbium-doped large-core fibre laser with 1.36 kW continuous-wave output power Opt. Express 12 6088-6092

[5] Alvarez-Chavez J A, Grudinin A B, Nilsson J, Turner P W and Clarkson W A 1999 Mode selection in high power cladding pumped fibre lasers with tapered section in Conference on Laser and Electro-Optics, OSA Technical Digest (Baltimore, MD, USA) Optical Society of America pp. 247–248

[6] Kir'yanov A V and Il'ichev N N 2011 Self-induced laser line sweeping in an ytterbium fibre laser with non-resonant Fabry Perot cavity Laser Phys. Lett. 8 305-312

[7] Lobach I A, Kablukov S I, Podivilov E V and Babin S A 2014 Self-scanned single-frequency operation of a fibre laser driven by a self-induced phase grating Laser Phys. Lett. 11 045103 (6pp)

[8] Peterka P, Navratil1 P, Maria J, Dussardier B, Slavik R, Honzatko P and Kubecek V 2012 Self-induced laser line sweeping in double-clad Yb-doped fibre-ring lasers Laser Phys. Lett. 9 445-450

[9] Hideur A, Chartier T, Ozkul C and Sanchez F 2000 Dynamics and stabilization of a high power side-pumped Yb-doped double-clad fibre laser Opt. Communications 186 311-317

[10] W. Guan and J. R. Marciante, "Complete elimination of self-pulsations in dual-clad ytterbium-doped fibre lasers at all pumping levels," Optics Lett. Vol. 34(6), pp. 815-817 (2009)

[11]B. N. Upadhyaya, A. Kuruvilla, U. Chkrvarty, M. R. Shenoy, K. Thyagarajan, and S. M. Oak, "Effect of laser linewidth and fibre length on self-pulsing dynamics and output stabilization of single-mode Yb-doped double-clad fibre laser," Appl. Optics, Vol. 49(12), pp. 2316-2325 (2010)

[12] Siegman A E 1986 Lasers ed Aidan Kelly (Mill Valley, CA) University Science Books.

[13] Zhang Z, Zhou X, Sui Z, Wang J, Li H, Liu Y and Liu Y 2009 Numerical analysis of stimulated inelastic scatterings in ytterbium doped double-clad fibre amplifier with multi-ns-duration and multi-hundred-kW peak-power output Opt. Communications 282 1186-1190

[14] Pask H M, Carman R J, Hanna D C, Tropper A C, Mackechnie C J, Barber P R and Dawes J M 1995 Ytterbium-Doped Silica Fibre Lasers: Versalite Sources for the 1-1.2 □m Region IEEE Journal of Selected Topics in Quantum Electronics 1 2-13

[15] Martinez-Rios A, Torres-Gomez I, Anzueto-Sanchez G and Selvas-Aguilar R 2008 Self-pulsing in a double-clad ytterbium fibre laser induced by high scattering loss Opt. Communications 281 663-667

[16] Martinez-Rios A, Anzueto-Sanchez G, Monzon-Hernandez D, Salceda-Delgado G and Castrellon-Uribe J 2014 Multiwavelength switching of an EDFL by using a fixed fibre-comb filter and a broadband tunable S-bent fibre filter Opt. Laser Technol 58 197-201

[17] Jiang Z and Marciante J R 2008 Impact of transverse spatial-hole burning on beam quality in large-mode-area Yb-doped fibres J. Opt. Soc. Am. B 25 247-254